DALTON
FULL PAPER

Carbon–fluorine bond activation in the reactions between 1,2-bis[bis-(2,6-difluorophenyl)phosphino]ethane and [{MCl(μ-Cl)(η^5-C_5Me_5)}$_2$] (M = Rh or Ir)

John Fawcett,[a] Steffi Friedrichs,[a] John H. Holloway,[a] Eric G. Hope,[a] Vickie McKee,[b] Mark Nieuwenhuyzen,[b] David R. Russell[a] and Graham C. Saunders *,†,[a,b]

[a] *Department of Chemistry, University of Leicester, Leicester, UK LE1 7RH*
[b] *School of Chemistry, The Queen's University of Belfast, David Keir Building, Belfast, UK BT9 5AG*

The new fluorine-containing diphosphine $(C_6H_3F_2$-2,6)$_2PCH_2CH_2P(C_6H_3F_2$-2,6)$_2$ **I** has been prepared and structurally characterized by single-crystal X-ray diffraction. The reaction between [{RhCl(μ-Cl)(η^5-C_5Me_5)}$_2$] and **I** in refluxing benzene yielded the cationic species [RhCl{η^5-C_5Me_3[(2-$CH_2C_6H_3F$-6)$P(C_6H_3F_2$-2,6)CH_2]$_2$-1,3}]$^+$, which was characterized as the BF_4^- salt **1**. The reaction involved the regiospecific activation of two C–F bonds and two C–H bonds and the formation of two C–C bonds. In contrast, the reaction between [{IrCl(μ-Cl)(η^5-C_5Me_5)}$_2$] and **I** did not involve C–F bond activation, but resulted in the formation of the dinuclear complex [{$IrCl_2$(η^5-C_5Me_5)[$P(C_6H_3F_2$-2,6)$_2CH_2$]}$_2$] **2**, the characterization of which was confirmed by the synthesis of the $(C_6F_5)_2PCH_2CH_2P(C_6F_5)_2$ analogue [{$IrCl_2$(η^5-C_5Me_5)[$P(C_6F_5)_2CH_2$]}$_2$] **3**. The complexes [MCl{$(C_6H_3F_2$-2,6)$_2PCH_2CH_2P(C_6H_3F_2$-2,6)$_2$}(η^5-C_5Me_5)]$^+BF_4^-$ (M = Rh **4** or Ir **5**), unlike their $(C_6F_5)_2PCH_2CH_2P(C_6F_5)_2$ analogues, did not undergo C–F and C–H bond activation and C–C bond formation on thermolysis. The structures of complexes **2**–**4** have been determined by single-crystal X-ray diffraction.

We have recently demonstrated that two *ortho* bonds of the diphosphine $(C_6F_5)_2PCH_2CH_2P(C_6F_5)_2$ (dfppe) can be activated under mild conditions by the transition-metal complexes [{MCl(μ-Cl)(η^5-C_5Me_5)}$_2$] (M = Rh or Ir) to form the cations [MCl{η^5-C_5Me_3[2-$CH_2C_6F_4P(C_6F_5)CH_2$]$_2$-1,3}]$^+$ in quantitative yield.[1,2] We are currently carrying out extensive investigations into these remarkable reactions to determine the mechanism. In particular, we anticipate that variation of the reagents will aid in our understanding of the reactions. One possible mechanism for the activation of C–F bonds involves single-electron transfer from an electron-rich source to the electron-accepting fluoroaromatic.[3] This type of mechanism is supported by ESR evidence from the reaction between *trans*-[PtH_2{P(*cyclo*-C_6H_{11})$_3$}$_2$] and C_6F_5CN.[4] The degree of fluorination of an aromatic ring strongly affects its electron-accepting ability, *i.e.* hexafluorobenzene is more electron-accepting than fluorobenzene.[5] Richmond and co-workers[6] have reported that the activation of one *ortho* C–F bond of the Schiff base $Me_2NCH_2CH_2N{=}CHC_6F_xH_{5-x}$ by a tungsten(0) complex occurs whatever the degree of fluorination (x = 1–5), provided there is at least one *ortho* C–F bond. In contrast, Crespo and co-workers[7] found that one C–F bond of the Schiff base $PhCH_2N{=}CHC_6F_xH_{5-x}$ is activated by a platinum(II) complex only when x > 2 and both *ortho* positions are fluorinated. Here, we report the reactions between [{MCl(μ-Cl)(η^5-C_5Me_5)}$_2$] (M = Rh or Ir) and the new diphosphine $(C_6H_3F_2$-2,6)$_2PCH_2CH_2P(C_6H_3F_2$-2,6)$_2$, which is fluorinated only in the *ortho* positions, to establish whether the degree of fluorination of the diphosphine is significant in our system.

Results and Discussion

Addition of $Cl_2PCH_2CH_2PCl_2$ to $Li^+[C_6H_3F_2$-2,6$]^-$, formed by addition of $LiBu^n$ to $C_6H_3BrF_2$-2,6 in diethyl ether at −78 °C afforded a dark red slurry, from which the new diphosphine $(C_6H_3F_2$-2,6)$_2PCH_2CH_2P(C_6H_3F_2$-2,6)$_2$ **I** was isolated by column chromatography in 40% yield. Compound **1** was obtained pure after recrystallization from diethyl ether and characterized by elemental analysis, high-resolution mass spectrometry and multinuclear NMR spectroscopies (Table 1). The ^{19}F-{^{1}H} and ^{31}P-{^{1}H} NMR spectra, recorded in $CDCl_3$ (Figs. 1 and 2), represent the A and X parts respectively of an $AA'X_4X'_4$ spin system. These have been successfully simulated using the values ^3J(PP′) = 47.2, ^3J(PF) = 30.1, ^6J(PF′) = 1.2 and

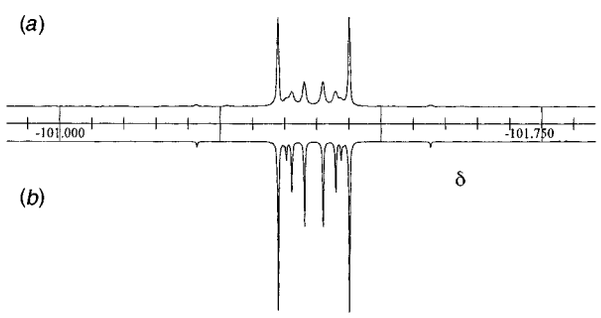

Fig. 1 Experimental (*a*) and simulated (*b*) ^{19}F-{^{1}H} NMR spectra of $(C_6H_3F_2$-2,6)$_2PCH_2CH_2P(C_6H_3F_2$-2,6)$_2$ **I**

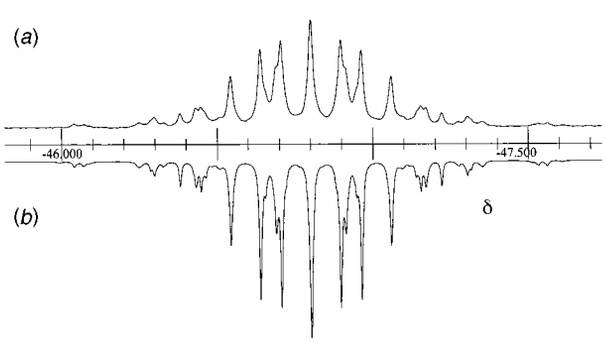

Fig. 2 Experimental (*a*) and simulated (*b*) ^{31}P-{^{1}H} NMR spectra of $(C_6H_3F_2$-2,6)$_2PCH_2CH_2P(C_6H_3F_2$-2,6)$_2$ **I**

† E-Mail: g.saunders@qub.ac.uk

Table 1 Analytical, mass spectral and NMR data for compounds **I** and **1**–**5**

Compound	Analysis (%)[a] and *m/z*	NMR[b]
I	C, 58.0 (57.6); H, 2.8 (3.0) 542 (M^+), 429 ($[M - C_6H_3F_2]^+$), 285 ($[M - 2C_6H_3F_2]^+$) [Found: 542.059 96. $C_{26}H_{16}F_8P_2$ (M^+) requires 542.059 95][c]	^{1}H: 7.26 (4 H, m, H_p), 6.80 [8 H, ddd, $^3J(H_mF) \approx {}^3J(H_mH_p)$ 8.2, $^4J(H_mP)$ 1.3, H_m], 2.53 [4 H, vt, $\frac{1}{2}$| ^2J(PH) + ^3J(PH)| 6.0, CH_2] ^{19}F-{^{1}H}: −101.39 (X part of an AA′X$_4$X′$_4$ spectrum) ^{31}P-{^{1}H}: −46.8 (A part of an AA′X$_4$X′$_4$ spectrum)
1	C, 44.1 (44.8); H, 3.55 (3.2)[d] 775 ($[M - BF_4]^+$), 739 ($[M - BF_4 - Cl - H]^+$), 627 ($[M - BF_4 - Cl - C_6H_3F_2]^+$)[e]	^{1}H: 7.44 (4 H, m), 6.87 (8 H, m), 4.40 [2 H, dm, ^2J(HH) 17.6, $C_6H_3FCH_2$], 4.01 [2 H, d, ^2J(HH) 17.6, $C_6H_3FCH_2$], 3.75 (2 H, m, CH_2), 3.42 (2 H, m, CH_2), 2.01 [6 H, d, ^4J(PH) 7.2, 4- and 5-CH_3], 1.27 (3 H, s, 2-CH_3) ^{19}F-{^{1}H}: −93.96 (2 F, s, $CH_2C_6H_3F$), −101.22 (4 F, br s, $C_6H_3F_2$), −152.50 (4 F, br s, BF_4^-) ^{31}P-{^{1}H}: 60.0 [d, ^1J(RhP) 139]
2[f]	C, 41.6 (41.3); H, 3.6 (3.4)	
3	C, 35.4 (35.5); H, 2.2 (2.2) 1384 ($[M - Cl - C_5Me_5]^+$), 1349 ($[M - 2Cl - C_5Me_5]^+$)[e]	^{1}H: 3.05 (4 H, s, CH_2), 1.39 (30 H, s, CH_3) ^{19}F: −125.90 [8 F, d, $^3J(F_oF_m)$ 20.4, F_o], −146.96 [4 F, t, $^3J(F_mF_p)$ 21.0, F_p], −159.23 (8 F, dd, F_m) ^{31}P-{^{1}H}: −23.3 (s)
4[g]	C, 48.7 (48.8); H, 3.8 (3.9); Cl, 3.4 (3.7) 815 ($[M - BF_4]^+$), 780 ($[M - BF_4 - Cl]^+$)[e]	^{1}H: 7.76 (2 H, m, H_p), 7.40 (2 H, m, H_p), 6.96 [4 H, dd, $^3J(H_mF) \approx {}^3J(H_mH_p)$ 8.5, H_m], 6.85 [4 H, dd, $^3J(H_mF) \approx {}^3J(H_mH_p)$ 9.0, H_m], 3.15 (2 H, m, CH_2), 2.91 (2 H, m, CH_2), 1.66 [15 H, t, ^4J(PH) 4.4, CH_3] ^{19}F-{^{1}H}: −96.02 (4 F, s), −97.65 (4 F, s), −154.66 and −154.71 (4 F, 2s, *ca.* 1:4, BF_4^-) ^{19}F-{^{1}H} [170 K, $(CD_3)_2CO$]: −93.50 (2 F, s, $C_6H_3F_2$), −96.99 (2 F, s, $C_6H_3F'_2$), −97.62 (2 F, s, $C_6H_3F'_2$), −98.11 (2 F, s, $C_6H_3F_2$) ^{31}P-{^{1}H}: 28.3 [d, ^1J(RhP) 147]
5	C, 43.2 (43.6); H, 2.8 (3.2) 905 ($[M - BF_4]^+$), 870 ($[M - BF_4 - Cl]^+$)[e]	^{1}H: 7.47 (2 H, m, H_p), 7.37 [2 H, tt, $^4J(H_pF) \approx {}^3J(H_mH_p)$ 7.2, H_p], 6.93 [4 H, dd, $^3J(H_mF) \approx {}^3J(H_mH_p)$ 8.0, H_m], 6.78 [4 H, dd, $^3J(H_mF) \approx {}^3J(H_mH_p)$ 9.3, H_m], 2.93 (4 H, m, CH_2), 1.37 [15 H, t, ^4J(PH) 4.4, CH_3] ^{19}F-{^{1}H}: −96.44 (4 F, s), −97.47 (4 F, s), −154.66 and −154.72 (4 F, 2s, *ca.* 1:4, BF_4^-) ^{19}F-{^{1}H} [210 K, $(CD_3)_2CO$]: −96.35 (2 F, s, $C_6H_3F_2$), −97.66 (2 F, s, $C_6H_3F'_2$), −98.57 (2 F, s, $C_6H_3F'_2$), −99.22 (2 F, s, $C_6H_3F_2$) ^{31}P-{^{1}H}: 1.0 (s)

[a] Required values are given in parentheses. [b] Unless stated otherwise, recorded in $CDCl_3$ at 298 K. Data given as chemical shift (δ) [relative intensity, multiplicity, *J*/Hz, assignment], s = singlet, d = doublet, t = triplet, vt = virtual triplet, m = multiplet. [c] EI. [d] Satisfactory analysis could not be obtained due to contamination by other salts, such as **4**, from which **1** could not be separated. [e] Positive-ion fast-atom bombardment with *m*-nitrobenzyl alcohol as matrix. [f] Insufficiently soluble for NMR. [g] Crystallized with 1 Me_2CO.

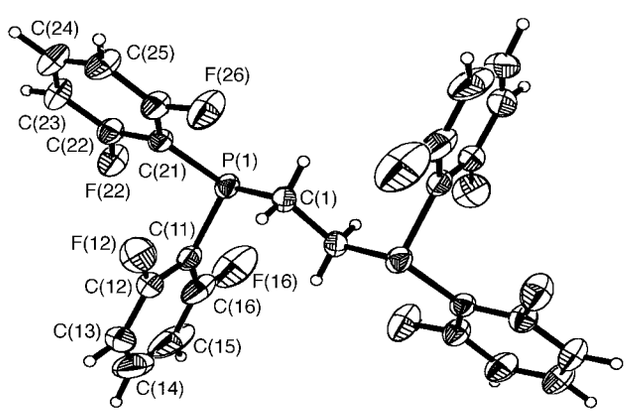

Fig. 3 Molecular structure of $(C_6H_3F_2\text{-}2,6)_2PCH_2CH_2P(C_6H_3F_2\text{-}2,6)_2$ **I**. Displacement ellipsoids are shown at the 30% probability level

$^9J(FF') = -0.4$ Hz (the signs are relative). The value of δ_P is similar to that of −44.4 for dfppe[8] recorded in $CDCl_3$, and the value of δ_F is similar to that of −101.47 for $P(C_6H_3F_2\text{-}2,6)_3$.[9] The absolute value of ^3J(PF) is similar to that of $PPh(C_6F_5)_2$,[9] but is considerably lower than those of *ca.* 40 Hz observed in the 2,6-difluorophenylphosphines $PPh_{3-x}(C_6H_3F_2\text{-}2,6)_x$ (x = 1–3).[9]

Diphosphine **I** was further characterized by single-crystal X-ray diffraction. The structure (Fig. 3) is very similar to those of dppe[10] and dfppe,[11] with the centre of the C(1)–C(1′) bond on a crystallographic centre of symmetry. Bond lengths and angles are listed in Table 2. The bond lengths and the P–C–C, C–P–C and C–C(P)–C angles are identical within experimental error of those of dfppe.[11] The most significant difference in the geometry about the phosphorus atoms between the two structures is the C(P)–C–F angles. For dfppe these angles lie in the range 118.8(3) to 121.4(4)° with an average of 120.2°, whereas the C(P)–C–F angles of **I** are more acute, lying in the range 116.9(2) to 118.9(2)° with an average of 117.7°.

Table 2 Bond lengths (Å) and angles (°) with estimated standard deviations (e.s.d.s) in parentheses for $(C_6H_3F_2\text{-}2,6)_2PCH_2CH_2P(C_6H_3F_2\text{-}2,6)$ **I**

P–C(1)	1.839(3)	C(1)–C(1′)	1.533(5)
P–C(11)	1.829(3)	P–C(21)	1.837(3)
C(11)–C(12)	1.375(5)	C(21)–C(22)	1.376(4)
C(12)–F(12)	1.354(5)	C(22)–F(22)	1.357(3)
C(12)–C(13)	1.369(6)	C(22)–C(23)	1.371(4)
C(13)–C(14)	1.366(11)	C(23)–C(24)	1.375(5)
C(14)–C(15)	1.331(12)	C(24)–C(25)	1.363(5)
C(15)–C(16)	1.376(8)	C(25)–C(26)	1.373(4)
C(16)–F(16)	1.356(6)	C(26)–F(26)	1.353(4)
C(16)–C(11)	1.391(5)	C(26)–C(21)	1.385(4)
P–C(1)–C(1′)	108.3(3)	C(1)–P–C(11)	99.09(13)
C(1)–P–C(21)	106.07(13)	C(11)–P–C(21)	100.53(12)
P–C(11)–C(12)	125.9(2)	P–C(21)–C(22)	118.0(2)
P–C(11)–C(16)	118.9(3)	P–C(21)–C(26)	128.7(2)
C(12)–C(11)–C(16)	115.2(4)	C(22)–C(21)–C(26)	113.0(2)
C(11)–C(12)–F(12)	117.6(3)	C(21)–C(22)–F(22)	116.9(2)
C(11)–C(12)–C(13)	123.6(5)	C(21)–C(22)–C(23)	125.5(3)
C(13)–C(12)–F(12)	118.8(5)	C(23)–C(22)–F(22)	117.6(3)
C(12)–C(13)–C(14)	118.3(7)	C(22)–C(23)–C(24)	117.9(3)
C(13)–C(14)–C(15)	120.8(7)	C(23)–C(24)–C(25)	120.2(3)
C(14)–C(15)–C(16)	120.6(7)	C(24)–C(25)–C(26)	118.9(3)
C(15)–C(16)–F(16)	121.2(5)	C(25)–C(26)–F(26)	116.6(3)
C(15)–C(16)–C(11)	121.5(6)	C(25)–C(26)–C(21)	124.5(3)
C(11)–C(16)–F(16)	117.3(4)	C(21)–C(26)–F(26)	118.9(2)

Treatment of $[\{RhCl(\mu\text{-}Cl)(\eta^5\text{-}C_5Me_5)\}_2]$ with **I** in refluxing benzene for 16 h afforded in high yield $[RhCl\{\eta^5\text{-}C_5Me_3$-

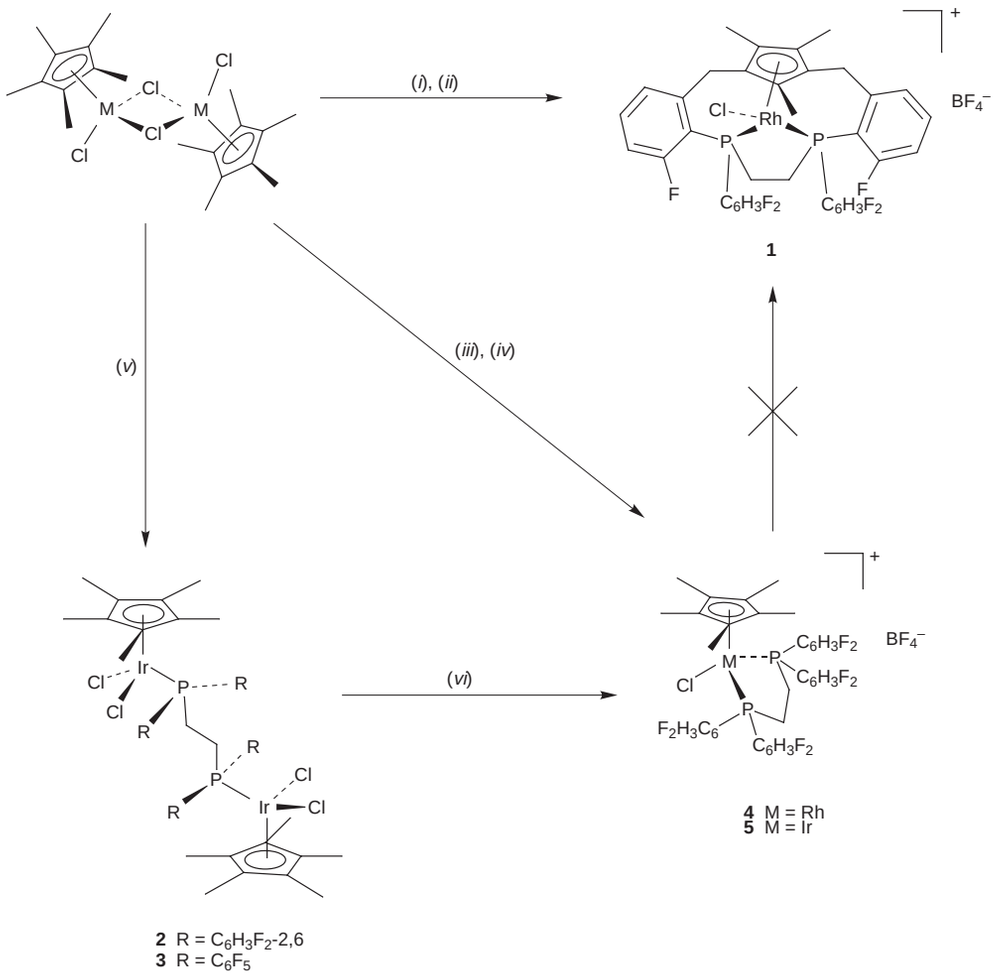

Scheme 1 (*i*) M = Rh, **I**, C_6H_6, heat; (*ii*) NH_4BF_4, Me_2CO; (*iii*) NH_4BF_4, MeOH; (*iv*) **I**, CH_2Cl_2; (*v*) M = Ir, **I** or dfppe, C_6H_6, heat; (*vi*) R = $C_6H_3F_2$-2,6, NH_4BF_4, Me_2CO

$[(2\text{-}CH_2C_6H_3F\text{-}6)P(C_6H_3F_2\text{-}2,6)CH_2]_2\text{-}1,3\}]^+Cl^-$ as an orange precipitate *via* C–F and C–H bond activation and concomitant C–C bond formation (Scheme 1). This product was characterized by mass spectrometry, which showed peaks at *m*/*z* 774 and 738 assigned to $[M - Cl - H]^+$ and $[M - 2Cl - 2H]^+$ respectively, but was found to be insoluble in all common organic solvents, precluding an NMR study. However, the tetrafluoroborate salt, **1**, formed by anion metathesis, is readily soluble in polar organic solvents. Salt **1** was characterized by elemental analysis, mass spectrometry and multinuclear NMR spectroscopies (Table 1). The NMR spectroscopic data indicate that **1** was contaminated by small amounts of similar complexes (such as **4**) from which it could not be separated, and this was confirmed by the analytical data which are not as required. The $^{31}P\text{-}\{^1H\}$ NMR spectrum, recorded in $CDCl_3$, exhibits a doublet of multiplets at δ 60.0 with an absolute value of $^1J(RhP)$ of 139 Hz. These values can be compared to those of δ 71.3 and 144 Hz for $[RhCl\{\eta^5\text{-}C_5Me_3[2\text{-}CH_2C_6F_4P(C_6F_5)CH_2]_2\text{-}1,3\}]^+Cl^-$ in the same solvent.[1] The ^1H NMR spectrum includes two multiplets at δ 7.44 and 6.87, with relative intensities 1 : 2, which are assigned to the twelve hydrogen atoms of the phenyl groups. There are four resonances between δ 3.0 and 4.5 of equal integral which are assigned to pairs of PCH_2 and $C_6H_3FCH_2$ methylene hydrogen atoms. Resonances assigned to PCH_2 occur as two multiplets with coupling to phosphorus. The hydrogen atoms of each PCH_2 moiety are *endo* and *exo* with respect to the cyclopentadienyl ring and, hence, are non-equivalent. Presumably, the equivalence of the two PCH_2 moieties arises due to the flexibility of the chelate ring. The resonances assigned to the $C_6H_3FCH_2$ methylene hydrogen atoms occur as a multiplet with coupling to phosphorus, as indicated by the $^1H\text{-}\{^{31}P\}$ NMR spectrum, and a doublet with a coupling to hydrogen, $^2J(HH)$, of 17.6 Hz. The 4- and 5-methyl hydrogen resonance is a doublet at δ 2.01 with a coupling to one phosphorus atom, $^4J(PH)$, of 7.2 Hz. The 2-methyl hydrogen resonance is a broad singlet at δ 1.27. The ^1H NMR spectrum is consistent with those of $[RhCl\{\eta^5\text{-}C_5Me_3\text{-}[2\text{-}CH_2C_6F_4P(C_6F_5)CH_2]_2\text{-}1,3\}]^+X^-$ ($X^- = Cl^-$ or BF_4^-).[1,2] The $^{19}F\text{-}\{^1H\}$ NMR spectrum exhibits a singlet at δ −93.96, which is assigned to the fluorine atoms of the two $CH_2C_6H_3F$ moieties, and a broad singlet at δ −101.22, which is assigned to the four fluorine atoms of the $C_6H_3F_2$ groups. This resonance is broadened due to hindered rotation about the P–C bond, as is found for $[RhCl\{\eta^5\text{-}C_5Me_3[2\text{-}CH_2C_6F_4P(C_6F_5)CH_2]_2\text{-}1,3\}]^+X^-$ ($X^- = Cl^-$ or BF_4^-).[1,2] Unfortunately, it was not possible to grow crystals of **1** suitable for X-ray diffraction.

In contrast to the reaction between $[\{RhCl(\mu\text{-}Cl)(\eta^5\text{-}C_5Me_5)\}_2]$ and **I**, treatment of $[\{IrCl(\mu\text{-}Cl)(\eta^5\text{-}C_5Me_5)\}_2]$ with 2 equivalents of **I** in refluxing benzene for 8 h did not cause activation of C–F bonds. Instead, the neutral dinuclear complex $[\{IrCl_2(\eta^5\text{-}C_5Me_5)[P(C_6H_3F_2\text{-}2,6)_2CH_2]\}_2]$ **2** was formed. No other phosphine-containing iridium species were detected in the reaction mixture. Complex **2** was characterized by elemental analysis (Table 1), but is not sufficiently soluble to permit an NMR study and the mass spectrum did not show the parent ion. The characterization of **3** was corroborated by the synthesis of the dfppe analogue $[\{IrCl_2(\eta^5\text{-}C_5Me_5)[P(C_6F_5)_2CH_2]\}_2]$ **3**, which was formed in quantitative yield on treatment of dfppe with 1.4 equivalents of $[\{IrCl(\mu\text{-}Cl)(\eta^5\text{-}C_5Me_5)\}_2]$ in refluxing benzene. Complex **3**, which is soluble in polar organic solvents, was characterized by elemental analysis and multinuclear NMR spectroscopies (Table 1), but, as for **2**, the mass spectrum did

Table 3 Selected bond distances (Å) and angles (°) with e.s.d.s in parentheses for $[\{IrCl_2(\eta^5\text{-}C_5Me_5)[P(C_6H_3F_2\text{-}2,6)_2CH_2]\}_2]\cdot 2Me_2CO$ **2**·$2Me_2CO$ and of $[\{IrCl_2(\eta^5\text{-}C_5Me_5)[P(C_6F_5)_2CH_2]\}_2]\cdot 2Me_2CO$ **3**·$2Me_2CO$[a]

		3·$2Me_2CO$	
	2·$2Me_2CO$	Molecule 1	Molecule 2[b]
Cp*–Ir	1.828(7)	1.825(7)	1.816(9)
Ir–P	2.334(3)	2.304(2)	2.306(3)
Ir–Cl	2.423(3), 2.397(3)	2.407(2), 2.388(2)	2.412(2), 2.404(2)
P–CH_2	1.817(11)	1.837(7)	1.896(14), 1.862(14)
CH_2–CH'_2	1.54(2)	1.524(14)	1.52(3), 1.50(3)
P–C (aryl)	1.831(12), 1.828(12)	1.855(7), 1.846(7)	1.90(2), 1.87(2)
			1.865(10), 1.865(10)
C(P)–C	1.40(2), 1.39(2)	1.396(10), 1.377(10)	1.40(2), 1.37(2)
	1.39(2), 1.41(2)	1.390(10), 1.386(10)	1.43(3), 1.34(3)
			1.32(2), 1.26(2)
			1.55(2), 1.52(3)
C–F (*ortho*)	1.356(14), 1.366(14)	1.353(9), 1.331(9)	1.36(2), 1.32(2)
	1.366(14), 1.340(13)	1.343(8), 1.339(9)	1.35(2), 1.33(2)
			1.38(2), 1.37(2)
			1.33(2), 1.28(3)
Cp*–Ir–P	136.4(3)	136.5(3)	137.0(3)
Cp*–Ir–Cl	124.5(3), 120.7(3)	123.5(3), 121.4(3)	124.1(3), 121.2(3)
P–Ir–Cl	90.75(11), 81.73(10)	90.63(7), 82.77(7)	89.73(10), 81.65(9)
Cl–Ir–Cl	88.66(3)	87.45(8)	88.49(9)
Ir–P–CH_2	112.2(4)	117.3(2)	124.9(5), 104.1(5)
P–CH_2–CH'_2	116.3(10)	112.3(6)	109.3(13), 106.8(13)
Ir–P–C (aryl)	121.0(4), 110.9(3)	120.5(2), 110.0(2)	130.3(5), 114.6(6)
			110.1(3), 110.1(3)
C (aryl)–P–CH_2	107.2(5), 99.5(5)	103.3(3), 99.9(3)	120.1(6), 96.5(6)
			95.6(6), 92.4(6)
C (aryl)–P–C (aryl)	104.7(5)	103.8(3)	111.0(7), 93.7(6)
P–C–C(F)	126.1(9), 121.0(9)	123.8(5), 120.3(6)	134.7(14), 109.8(13)
	125.4(9), 121.0(8)	126.2(6), 118.5(5)	125.4(14), 117(2)
			111.6(13), 110.8(11)
			136.6(10), 124.9(12)
C(P)–C–F	117.9(10), 118.2(10)	122.2(7), 119.8(7)	122(2), 119.7(14)
	119.9(10), 116.8(10)	121.0(7), 120.3(6)	122(2), 121(2)
			133(2), 130(2)
			112(2), 111(2)
C(F)–C(P)–C(F)	112.2(11), 113.3(10)	115.7(7), 115.1(7)	115(2), 117(2)
			137(2), 98.4(14)

[a] Cp* denotes the cyclopentadienyl centroid. [b] Some of the bond lengths and angles for this molecule are given as pairs due to disorder of the C_6F_5 rings and the CH_2 atoms. The relevant atoms were modelled for two sites with 50% occupancy and refined as isotropic.

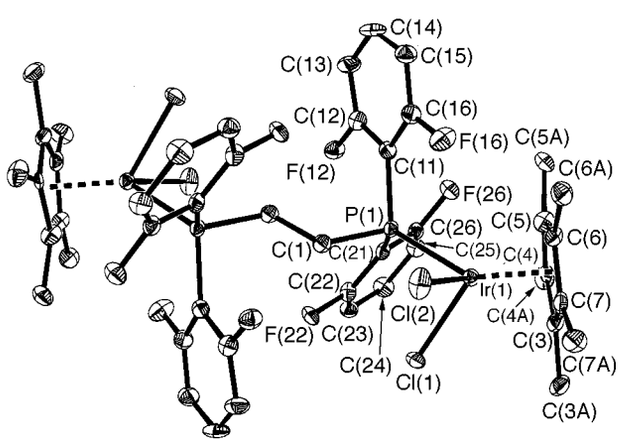

Fig. 4 Molecular structure of $[\{IrCl_2(\eta^5\text{-}C_5Me_5)[P(C_6H_3F_2\text{-}2,6)_2CH_2]\}_2]$ **2**. Displacement ellipsoids are shown at the 30% probability level. The hydrogen atoms are omitted for clarity

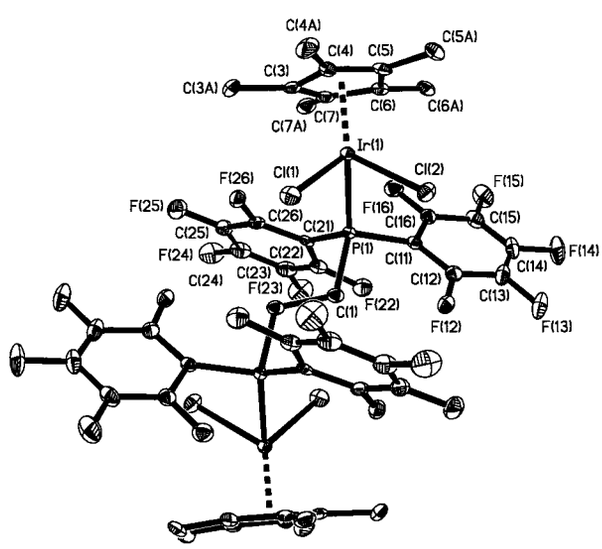

Fig. 5 Molecular structure of one of the independent molecules of $[\{IrCl_2(\eta^5\text{-}C_5Me_5)[P(C_6F_5)_2CH_2]\}_2]$ **3**. Details as in Fig. 4

not show the parent ion. Complexes **2** and **3** were structurally characterized by single-crystal X-ray diffraction. Attempts to prepare $[\{RhCl_2(\eta^5\text{-}C_5Me_5)[P(C_6F_5)_2CH_2]\}_2]$ by similar methods have been unsuccessful, leading only to the formation of $[RhCl\{\eta^5\text{-}C_5Me_3[2\text{-}CH_2C_6F_4P(C_6F_5)CH_2]_2\text{-}1,3\}]^+X^-$, even when a large excess of $[\{RhCl(\mu\text{-}Cl)(\eta^5\text{-}C_5Me_5)\}_2]$ was used.

The structures of complexes **2** and **3** are shown in Figs. 4 and 5 respectively and selected bond lengths and angles are given in Table 3. The structure of **3** comprises two crystallographically

Table 4 Selected bond distances (Å) and angles (°) with e.s.d.s in parentheses for $[RhCl\{(C_6H_3F_2\text{-}2.6)_2PCH_2CH_2P(C_6H_3F_2\text{-}2.6)_2\}(\eta^5\text{-}C_5Me_5)]^+BF_4^-\cdot Me_2CO$ **4**·Me_2CO

Cp*–Rh	1.868(4)	Rh–Cl	2.385(1)
Rh–P(1)	2.329(1)	Rh–P(2)	2.349(1)
P(1)–C(1)	1.913(11)	P(1)–C(1′)	1.784(11)
P(2)–C(2)	1.782(8)	P(2)–C(2′)	1.961(8)
C(1)–C(2)	1.529(13)	C(1b)–C(2′)	1.530(11)
P(1)–C(11)	1.843(4)	P(1)–C(21)	1.826(5)
P(2)–C(31)	1.833(6)	P(2)–C(41)	1.833(4)
C(11)–C(12)	1.397(7)	C(21)–C(22)	1.396(7)
C(11)–C(16)	1.387(7)	C(21)–C(26)	1.385(8)
C(12)–F(12)	1.355(7)	C(22)–F(22)	1.347(8)
C(16)–F(16)	1.362(6)	C(26)–F(26)	1.354(6)
C(31)–C(32)	1.384(9)	C(41)–C(42)	1.387(7)
C(31)–C(36)	1.404(7)	C(41)–C(46)	1.376(6)
C(32)–F(32)	1.344(6)	C(42)–F(42)	1.343(7)
C(36)–F(36)	1.351(9)	C(46)–F(46)	1.363(5)
Cp*–Rh–Cl	120.1(14)	Cp*–Rh–P(1)	131.6(13)
Cp*–Rh–P(2)	135.5(13)	Cl–Rh–P(1)	82.20(4)
Cl–Rh–P(2)	87.10(4)	P(1)–Rh–P(2)	83.00(5)
Rh–P(1)–C(11)	123.9(2)	Rh–P(1)–C(21)	114.7(2)
Rh–P(1)–C(1)	107.2(3)	Rh–P(1)–C(1′)	105.7(3)
Rh–P(2)–C(31)	122.0(2)	Rh–P(2)–C(41)	118.70(14)
Rh–P(2)–C(2)	108.0(3)	Rh–P(2)–C(2′)	104.7(3)
C(11)–P(1)–C(1)	91.1(4)	C(11)–P(1)–C(1′)	106.2(4)
C(21)–P(1)–C(1)	115.5(4)	C(21)–P(1)–C(1′)	101.1(4)
C(11)–P(1)–C(21)	102.8(2)	C(31)–P(2)–C(2)	88.7(4)
C(31)–P(2)–C(2′)	110.9(4)	C(41)–P(2)–C(2)	116.6(3)
C(41)–P(2)–C(2′)	98.7(3)	C(31)–P(2)–C(41)	99.5(2)
P(1)–C(11)–C(12)	122.1(4)	C(11)–C(12)–F(12)	118.5(4)
P(1)–C(11)–C(16)	123.3(4)	C(11)–C(16)–F(16)	118.5(4)
C(12)–C(11)–C(16)	114.0(4)	P(1)–C(21)–C(22)	126.3(5)
C(21)–C(22)–F(22)	119.2(6)	P(1)–C(21)–C(26)	120.2(4)
C(21)–C(26)–F(26)	118.0(4)	C(22)–C(21)–C(26)	113.5(5)
P(2)–C(31)–C(32)	126.0(4)	C(31)–C(32)–F(32)	119.3(5)
P(2)–C(31)–C(36)	120.4(5)	C(31)–C(36)–F(36)	117.8(6)
C(32)–C(31)–C(36)	113.5(5)	P(2)–C(41)–C(42)	128.5(4)
C(41)–C(42)–F(42)	118.8(5)	P(2)–C(41)–C(46)	118.7(3)
C(41)–C(46)–F(46)	116.8(4)	C(42)–C(41)–C(46)	113.2(4)

independent molecules in the unit cell, one of which shows disordered C_6F_5 rings and disordered methylene carbon atoms. Both molecules of **3** possess similar bond angles and distances about the iridium atom. For complex **2** and both molecules of **3** the centre of each $H_2C–CH_2$ bond lies on a crystallographic centre of symmetry and, thus, there is a *trans* arrangement about the C–C bond. The geometry about the iridium atoms is that of a three-legged piano stool with the P–Ir–Cl and Cl–Ir–Cl angles lying in the range 81.65(9) to 90.75(11)°. The $Cp^*_{centroid}$–Ir–Cl angles lie in the range 120.7(3) to 124.5(3)°, and the $Cp^*_{centroid}$–Ir–P angles are *ca.* 136.5°, consistent with the structures of other $[IrCl_2(PR_3)(\eta^5\text{-}C_5Me_5)]$ complexes.[12,13] The $Cp^*_{centroid}$–Ir distances of **2** and **3** are the same within experimental error and the Ir–Cl distances are similar. The Ir–P distance of **2** is *ca.* 0.03 Å longer than those of **3**, which are significantly longer than the values of 2.281(7) and 2.211(2) Å for $[IrCl_2(PMe_3)(\eta^5\text{-}C_5Me_5)]$[12] and $[IrCl_2\{P(OC_6H_3F_2\text{-}2,6)_3\}(\eta^5\text{-}C_5Me_5)]$[13] respectively. The Ir–P bond lengths in $[IrCl_2(PX_3)(\eta^5\text{-}C_5Me_5)]$ complexes would be expected to decrease with increasing π-acceptor strength of the phosphorus ligands, which follows the order of substituents, X, Ph < Me < OR < C_6F_5.[14] For electronic reasons alone, it is anticipated that the Ir–P bond length of **3** should be shorter than that of $[IrCl_2\{P(OC_6H_3F_2\text{-}2,6)_3\}(\eta^5\text{-}C_5Me_5)]$. The length of the Ir–P bond of **3** is, therefore, evidently a consequence of the bulk of the ligand. The longer Ir–P bond of **2** may be a consequence of both the lower π-acceptor strength and the greater steric pressure, induced by the more acute C(P)–C–F angles, of **I** compared to dfppe. It has been shown that the σ-donor and π-acceptor properties of the 2,6-difluorophenylphosphines $P(C_6H_3F_2\text{-}2,6)_3$, $PPh(C_6H_3F_2\text{-}2,6)_2$ and $PPh_2(C_6H_3F_2\text{-}2,6)$ closely resemble those of $P(C_6F_5)_3$, $PPh(C_6F_5)_2$ and $PPh_2(C_6F_5)$ respectively,[9] suggesting that it is the steric effect which dominates. It is also noted that the mean Ir–Cl distances in **2** (2.41 Å) and **3** (2.40 Å) are slightly larger than the values of 2.37 and 2.38 Å for $[IrCl_2(PMe_3)(\eta^5\text{-}C_5Me_5)]$[12] and $[IrCl_2\{P(OC_6H_3F_2\text{-}2,6)_3\}(\eta^5\text{-}C_5Me_5)]$[13] respectively. The bond lengths and angles of the diphosphine ligand in **2** are the same as for **I**, except for the C (aryl)–P–C (aryl) and P–CH_2–CH'_2 angles which are larger for **2** by *ca.* 4 and 7° respectively and the C(P)–C–F angles which have a slightly larger mean value of 118.2°. The bond lengths and angles for the dfppe ligand in the non-disordered molecule of **3** are similar to those of dfppe,[11] except for the C (aryl)–P–C (aryl) and P–CH_2–CH'_2 angles which are larger for **3** by *ca.* 4 and 3° respectively.

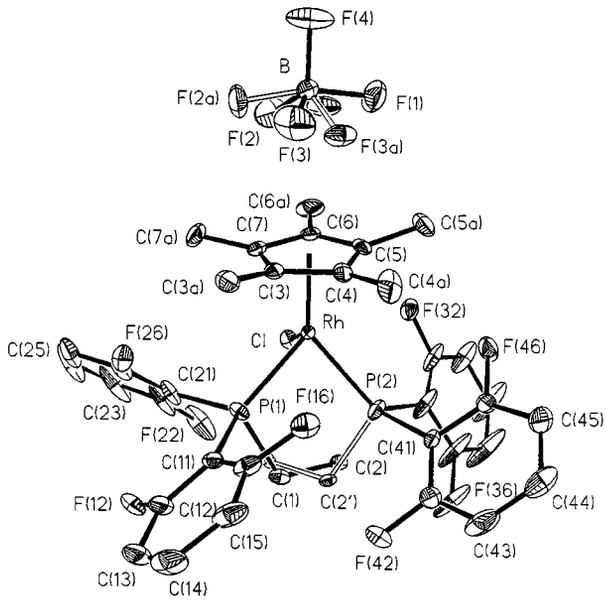

Fig. 6 Molecular structure of $[RhCl\{(C_6H_3F_2\text{-}2,6)_2PCH_2CH_2P(C_6H_3F_2\text{-}2,6)_2\}(\eta^5\text{-}C_5Me_5)]^+BF_4^-$ **4**. Details as in Fig. 4

The cations $[MX\{(C_6F_5)_2PCH_2CH_2P(C_6F_5)_2\}(\eta^5\text{-}C_5Me_5)]^+$ have been shown to be intermediates in the reactions between $[\{MX(\mu\text{-}X)(\eta^5\text{-}C_5Me_5)\}_2]$ and dfppe in both ethanol (M = Rh, X = Cl or Br; M = Ir, X = Cl)[2,15] and benzene (M = Rh, X = Br),[15] and it would be reasonable to assume that an analogous cation is an intermediate in the reaction between $[\{RhCl(\mu\text{-}Cl)(\eta^5\text{-}C_5Me_5)\}_2]$ and **I**. The tetrafluoroborate salts $[MCl\{(C_6H_3F_2\text{-}2,6)_2PCH_2CH_2P(C_6H_3F_2\text{-}2,6)_2\}(\eta^5\text{-}C_5Me_5)]^+BF_4^-$ (M = Rh **4** or Ir **5**) were synthesized by addition of **I** to solutions of $[\{MCl(\mu\text{-}Cl)(\eta^5\text{-}C_5Me_5)\}_2]$ and NH_4BF_4 in methanol. The iridium salt **5** was also formed on addition of NH_4BF_4 to complex **2** (Scheme 1). Salts **4** and **5** were characterized by elemental analysis, mass spectrometry and multinuclear NMR spectroscopies (Table 1). The $^{31}P\text{-}\{^1H\}$ NMR spectrum of **4** exhibits a doublet at δ 28.3 with a rhodium–phosphorus coupling $^1J(RhP)$ of 147 Hz, consistent with the values of δ 35.1 and 150.5 Hz for $[RhCl\{(C_6F_5)_2PCH_2CH_2P(C_6F_5)_2\}(\eta^5\text{-}C_5Me_5)]^+BF_4^-$ **6**.[2] The $^{31}P\text{-}\{^1H\}$ NMR spectrum of **5** exhibits a singlet resonance at δ 1.0 consistent with that of $[IrCl\{(C_6F_5)_2PCH_2CH_2P(C_6F_5)_2\}(\eta^5\text{-}C_5Me_5)]^+BF_4^-$ at δ 9.8.[2] Variable-temperature $^{19}F\text{-}\{^1H\}$ NMR spectroscopic studies of **4** and **5** in $(CD_3)_2CO$ indicate that for each complex cation the $C_6H_3F_2$ groups of each $P(C_6H_3F_2\text{-}2,6)_2$ moiety are non-equivalent and there is hindered rotation about both pairs of P–$C_6H_3F_2$ bonds. The activation energies for rotation, $\Delta G^{\ddagger}$, are calculated to be 33 ± 2 and 43 ± 2 kJ mol^{-1} for **4** and 42 ± 2 and 46.5 ± 3 kJ mol^{-1} for **5**. These are the same within experimental error as the respective values for $[MCl\{(C_6F_5)_2PCH_2CH_2P(C_6F_5)_2\}(\eta^5\text{-}C_5Me_5)]^+BF_4^-$ (M = Rh or Ir).[2] In addition, the structure of salt **4** (Fig. 6) was determined by single-crystal X-ray diffraction. Selected bond distances and angles for **4** are presented in

Table 4. The structure of the cation of **4** is of the three-legged piano-stool type similar to that of the cation of **6**.[2] The Rh–Cl and $Cp^*_{centroid}$–Rh distances and the respective $Cp^*_{centroid}$–Rh–X angles of **4** and **6** are identical within experimental error. However, there are some significant differences in the bond lengths and angles about the rhodium atom. In particular, the Rh–P distances of **4** are *ca.* 0.02 Å shorter than those of **6** [2.362(2) and 2.342(2) Å] and, consequently, the P–Rh–P angle is *ca.* 1° more acute in **4**. Comparison of the Rh–P distances and variable-temperature NMR data of **4** with those of **6** suggest that the ligand **I** is sterically less demanding than dfppe in these complexes, allowing a closer approach of the phosphorus atoms to the rhodium without leading to more restricted rotation about the P–C bonds. It is unclear as to how this arises since the P–C (aryl), PC–C and C–F bond lengths and P–C–C and PC–C–F bond angles of **4** are the same within experimental error as the analogous bond lengths and angles of **6**, which might be expected to lead to the ligands displaying similar steric properties. It is also noted that the order of the Rh–P distances of **4** and **6** is opposite to that for the Ir–P distances of **2** and **3**.

The cation of complex **4**, similar to that of **6**, possesses some short F···CH_3 distances. In particular, F(26)···C(3a), F(32)···C(5a) and F(46)···C(5a) are 3.102, 3.032 and 3.061 Å respectively. There are a number of short F···CH_3 and F···C(CH_3) distances between fluorine atoms of the tetrafluoroborate anion and carbon atoms of the pentamethylcyclopentadienyl ring. In particular, F(1)···C(1), F(1a)···C(6), F(2)···C(7), F(3a)···C(4) and F(3a)···C(4a) are 3.109, 3.014, 3.013, 2.971 and 3.043 Å respectively. Furthermore, there are four short distances between the anion and aryl carbon atoms of other cations: F(1a)···C(15), F(2a)···C(45), F(3)···C(33) and F(3)···C(34) are 3.056, 2.898, 2.988 and 2.965 Å respectively. However, in contrast to the established reactivity of $[MCl\{(C_6F_5)_2PCH_2CH_2P(C_6F_5)_2\}(\eta^5\text{-}C_5Me_5)]^+BF_4^-$ (M = Rh or Ir),[2] neither **4** nor **5** underwent C–F and C–H bond activation and C–C bond formation on thermolysis in ethanol.

Conclusion

We have demonstrated that the reaction between the diphosphine $(C_6H_3F_2\text{-}2,6)_2PCH_2CH_2P(C_6H_3F_2\text{-}2,6)_2$ and $[\{MCl(\mu\text{-}Cl)(\eta^5\text{-}C_5Me_5)\}_2]$ in benzene proceeds differently for M = Rh and M = Ir. In the former case activation of two *ortho* C–F bonds occurs to yield the cation $[RhCl\{\eta^5\text{-}C_5Me_3[(2\text{-}CH_2C_6H_3F\text{-}6)P(C_6H_3F_2\text{-}2,6)CH_2]_2\text{-}1,3\}]^+$. In the latter case no C–F bond activation is observed and the product is a dinuclear complex comprising a bridging disphosphine, $[\{IrCl_2(\eta^5\text{-}C_5Me_5)[P(C_6H_3F_2\text{-}2,6)_2CH_2]\}_2]$. It is not clear as to why these reactions should give very different products, but it is noted that the reactions between $(C_6F_5)_2PCH_2CH_2P(C_6F_5)_2$ and an excess of $[\{MCl(\mu\text{-}Cl)(\eta^5\text{-}C_5Me_5)\}_2]$ (M = Rh or Ir) give the activated $[RhCl\{\eta^5\text{-}C_5Me_3[CH_2C_6F_4P(C_6F_5)CH_2]_2\text{-}1,3\}]^+$ and the bridged $[\{IrCl_2(\eta^5\text{-}C_5Me_5)[P(C_6F_5)_2CH_2]\}_2]$ respectively as the only products. It is also noted that the M–P distances of $[RhCl\{(C_6F_5)_2PCH_2CH_2P(C_6F_5)_2\}(\eta^5\text{-}C_5Me_5)]^+BF_4^-$ are *longer* than those of $[RhCl\{(C_6H_3F_2\text{-}2,6)_2PCH_2CH_2P(C_6H_3F_2\text{-}2,6)_2\}(\eta^5\text{-}C_5Me_5)]^+BF_4^-$, whereas the M–P distance of $[\{IrCl_2(\eta^5\text{-}C_5Me_5)[P(C_6F_5)_2CH_2]\}_2]$ is *shorter* than that of $[\{IrCl_2(\eta^5\text{-}C_5Me_5)[P(C_6H_3F_2\text{-}2,6)_2CH_2]\}_2]$. These differences may be a consequence of the steric differences between $(C_6H_3F_2\text{-}2,6)_2PCH_2CH_2P(C_6H_3F_2\text{-}2,6)_2$ and $(C_6F_5)_2PCH_2CH_2P(C_6F_5)_2$, caused by the more acute C(P)–C–F angles of the former.

The lack of C–F bond activation on thermolysis of $[MCl\{(C_6H_3F_2\text{-}2,6)_2PCH_2CH_2P(C_6H_3F_2\text{-}2,6)_2\}(\eta^5\text{-}C_5Me_5)]^+BF_4^-$ (M = Rh or Ir) in ethanol may be ascribed to electronic differences between $(C_6H_3F_2\text{-}2,6)_2PCH_2CH_2P(C_6H_3F_2\text{-}2,6)_2$ and $(C_6F_5)_2PCH_2CH_2P(C_6F_5)_2$ and is not inconsistent with an electron-transfer mechanism. We are carrying out further studies into the C–F bond activation process in these intriguing reactions in order to elucidate the mechanisms.

Experimental

Physical measurements

The ^1H, ^{19}F and ^{31}P NMR spectra were recorded using Bruker ARX250, DPX300 or DRX400 spectrometers; ^1H (250.13, 300.01 or 400.13 MHz) were referenced internally using the residual protio solvent resonance relative to $SiMe_4$ (δ 0), ^{19}F (235.36, 282.26 or 376.50 MHz) externally to $CFCl_3$ (δ 0) and ^{31}P (101.26, 121.45, 161.98 MHz) externally to 85% H_3PO_4 (δ 0). All chemical shifts are quoted in δ (ppm), using the high frequency positive convention, and coupling constants in Hz. The NMR simulations were performed using the gNMR simulation package.[16] Position-ion FAB mass spectra were recorded on a Kratos Concept 1H mass spectrometer. Elemental analyses were carried out by Butterworths Ltd. or by A.S.E.P., The School of Chemistry, The Queen's University of Belfast.

Materials

The compounds $Cl_2PCH_2CH_2PCl_2$, $[\{MCl(\mu\text{-}Cl)(\eta^5\text{-}C_5Me_5)\}_2]$ (M = Rh or Ir) (Aldrich), NH_4BF_4 (BDH), $C_6H_3BrF_2$-2,6 and $(C_6F_5)_2PCH_2CH_2P(C_6F_5)_2$ (Fluorochem) were used as supplied. Diethyl ether was dried by distillation under nitrogen from over sodium. Light petroleum (b.p. 40–60 °C) was used throughout.

Preparations

$(C_6H_3F_2\text{-}2,6)_2PCH_2CH_2P(C_6H_3F_2\text{-}2,6)_2$ I. A 1.6 M solution of $LiBu^n$ in hexane (48.8 cm^3, 0.078 mol) was diluted with diethyl ether (25 cm^3) and added during 2 h to $C_6H_3BrF_2$-2,6 (20.48 g, 0.104 mol) in diethyl ether at −78 °C. The mixture was stirred at −78 °C for 3 h. A solution of $Cl_2PCH_2CH_2PCl_2$ (1.95 cm^3, 0.013 mol) in diethyl ether (50 cm^3) was added during 1 h, during which time the mixture darkened. The mixture was allowed to warm to room temperature over 12 h. The resulting dark red slurry was washed with 20% NH_4Cl(aq) (200 cm^3), 10% NH_4Cl(aq) (200 cm^3) and water (2 × 200 cm^3). The organic layer was separated, dried over anhydrous $MgSO_4$ and filtered. The solvent was removed by rotary evaporation and the product purified by column chromatography and recrystallization from diethyl ether to afford colourless crystals of **I**. Yield 2.77 g (40%).

$[RhCl\{\eta^5\text{-}C_5Me_3[(2\text{-}CH_2C_6H_3F\text{-}6)P(C_6H_3F_2\text{-}2,6)CH_2]_2\text{-}1,3\}]^+BF_4^-$ 1. A slurry of $[\{RhCl(\mu\text{-}Cl)(\eta^5\text{-}C_5Me_5)\}_2]$ (0.10 g, 0.16 mmol) and compound **I** (0.18 g, 0.32 mmol) in benzene (50 cm^3) was refluxed under nitrogen for 16 h, during which time an orange precipitate of the chloride salt of **1** was formed. The solid was filtered off and washed with light petroleum. Yield 0.21 g (81%). The salt was slurried in acetone (30 cm^3) and NH_4BF_4 (1.0 g, 9.5 mmol) added. After 16 h the solvent was removed by rotary evaporation and the solid extracted into dichloromethane. The extract was filtered and the solvent removed by rotary evaporation to afford **1** as a yellow solid, which was dried *in vacuo*.

$[\{IrCl_2(\eta^5\text{-}C_5Me_5)[P(C_6H_3F_2\text{-}2,6)_2CH_2]\}_2]$ 2. A slurry of $[\{IrCl(\mu\text{-}Cl)(\eta^5\text{-}C_5Me_5)\}_2]$ (0.10 g, 0.13 mmol) and compound **I** (0.18 g, 0.32 mmol) in benzene (50 cm^3) was refluxed under nitrogen for 8 h. After cooling, the resultant yellow precipitate was filtered off and recrystallized from acetone–light petroleum to afford yellow crystals of **2**. Yield 0.10 g (57%).

$[\{IrCl_2(\eta^5\text{-}C_5Me_5)[P(C_6F_5)_2CH_2]\}_2]$ 3. A slurry of $[\{IrCl(\mu\text{-}Cl)(\eta^5\text{-}C_5Me_5)\}_2]$ (0.14 g, 0.18 mmol) and dfppe (0.10 g, 0.13 mmol) in benzene (50 cm^3) was refluxed under nitrogen for 8 h to yield a orange solution. The solvent was removed by rotary

Table 5 X-Ray crystallographic data collection, solution and refinement details[a] for $(C_6H_3F_2\text{-}2,6)_2PCH_2CH_2P(C_6H_3F_2\text{-}2,6)_2$ **I**, $[\{IrCl_2(\eta^5\text{-}C_5Me_5)[P(C_6H_3F_2\text{-}2,6)_2CH_2]\}_2]\cdot 2Me_2CO$ **2**·$2Me_2CO$, $[\{IrCl_2(\eta^5\text{-}C_5Me_5)[P(C_6F_5)_2CH_2]\}_2]\cdot 2Me_2CO$ **3**·$2Me_2CO$ and $[RhCl\{(C_6H_3F_2\text{-}2,6)_2PCH_2CH_2P(C_6H_3F_2\text{-}2,6)_2\}(\eta^5\text{-}C_5Me_5)]^+BF_4^-\cdot Me_2CO$ **4**·Me_2CO

	I	**2**	**3**	**4**
Formula	$C_{26}H_{16}F_8P_2$	$C_{26}H_{29}Cl_2F_4IrOP$	$C_{52}H_{46}Cl_4F_{20}Ir_2O_2P_2$	$C_{39}H_{37}BClF_{12}OP_2Rh$
M	542.33	727.56	1671.03	960.80
Crystal system	Triclinic	Monoclinic	Triclinic	Monoclinic
Space group	$P\bar{1}$	$P2_1/n$	$P\bar{1}$	$P2_1/n$
a/Å	7.372(1)	9.983(2)	12.149(2)	10.938(1)
b/Å	9.458(1)	16.220(5)	12.650(3)	20.915(1)
c/Å	9.846(1)	16.605(3)	19.663(4)	17.352(1)
α/°	117.15(1)	—	86.30(2)	—
β/°	93.32(1)	99.95(3)	79.36(2)	101.681(6)
γ/°	98.07(1)	—	78.87(2)	—
U/Å^3	598.99(12)	2648.5(11)	2913.0(11)	3887.5(4)
Z	1	4	2	4
T/K	293	186	153	153
μ/mm^{-1}	0.257	5.350	4.906	0.68
Total data	2254	6920	10 772	7641
Unique data, R_{int}	1780, 0.073	5485, 0.0428	10 249, 0.0240	6831, 0.0370
$R1$, $wR2$ $[I > 2\sigma(I)]$[b]	0.0474, 0.1209	0.0617, 0.1450	0.0429, 0.0827	0.0422, 0.0931
(all data)	0.0543, 0.1261	0.0880, 0.1902	0.0640, 0.0916	0.0535, 0.1040

[a] Details in common: Siemens P4 diffractometer, λ(Mo-Kα) = 0.710 73 Å, graphite monochromator, scan type ω. [b] $R1 = \Sigma||F_o| - |F_c||/\Sigma|F_o|$; $wR2 = [\Sigma w(F_o^2 - F_c^2)^2/\Sigma w(F_o^2)^2]^{\frac{1}{2}}$.

evaporation and the solid recrystallized from acetone–light petroleum. Yield *ca.* 0.2 g (*ca.* 100%).

$[RhCl\{(C_6H_3F_2\text{-}2,6)_2PCH_2CH_2P(C_6H_3F_2\text{-}2,6)_2\}(\eta^5\text{-}C_5Me_5)]^+BF_4^-$ 4. The salt NH_4BF_4 (1.0 g, 9.5 mmol) was added to $[\{RhCl(\mu\text{-}Cl)(\eta^5\text{-}C_5Me_5)\}_2]$ (0.10 g, 0.16 mmol) in methanol (40 cm^3). After 20 min compound **I** (0.18 g, 0.32 mmol) in dichloromethane (20 cm^3) was added and the mixture stirred for 2 h. The solvent was removed by rotary evaporation and the orange solid extracted into dichloromethane and filtered through Celite. The solvent was removed by rotary evaporation and the solid recrystallized from acetone–light petroleum to afford orange crystals of **4**·Me_2CO. Yield 0.13 g (42%).

$[IrCl\{(C_6H_3F_2\text{-}2,6)_2PCH_2CH_2P(C_6H_3F_2\text{-}2,6)_2\}(\eta^5\text{-}C_5Me_5)]^+BF_4^-$ 5. The compounds $[\{IrCl(\mu\text{-}Cl)(\eta^5\text{-}C_5Me_5)\}_2]$ (0.10 g, 0.13 mmol), NH_4BF_4 (1.0 g, 9.5 mmol) and **I** (0.18 g, 0.32 mmol) were treated as for **4**. The product was obtained as a lemon-yellow crystalline solid. Yield 0.19 g (76%).

Crystallography

Crystals of compounds **I** and **2**, suitable for diffraction, were grown from $CDCl_3$–light petroleum and acetone–light petroleum respectively, those of **3** and **4** from acetone. The crystal data and experimental parameters for the compounds are given in Table 5. Unit-cell parameters for **I** were determined from the optimized setting angles of 38 reflections in the range $5.1 < \theta < 12.5°$, for **2** from 23 reflections in the range $5.1 < \theta < 12.6°$, for **3** from 35 reflections in the range $5.0 < \theta < 12.5°$ and for **4** from 36 reflections in the range $5.3 < \theta < 12.6°$. A semiempirical absorption correction was applied to the data for **3** and **4** (based on ψ scans), and the data were corrected for Lorentz-polarization effects. Crystal stability was monitored by the observation of the intensities of three standard check reflections; for no structure was there any loss of intensity.

The structure of compound **I** was solved by direct methods and refined on F^2 using SHELXL 96.[17] Only one molecule is found in the unit cell, with the centre of the C–C bond linking the two phosphorus atoms on a centre of symmetry. All non-hydrogen atoms were refined with anisotropic displacement parameters. The hydrogen atoms bonded to C(1) were included in calculated positions (C–H 0.96 Å) with a fixed isotropic displacement parameter $1.2U_{eq}$ of C(1).

The structure of complex **2** was solved by Patterson and Fourier methods and refined on F^2 using SHELXL 96.[17] All non-hydrogen atoms were refined with anisotropic displacement parameters. All hydrogen atoms were included in calculated positions (C–H 0.96 Å) with a fixed isotropic displacement parameter $1.5U_{eq}$(C) for the methyl groups and $1.2U_{eq}$(C) for the remainder. All crystals examined exhibited split diffraction peaks and the data resulting from the best crystal were scanned and 46 suspect reflections rejected. Analytical and empirical absorption corrections did not improve the R factors or residual electron-density peaks from refinement with uncorrected data, and a correction based on the method of Blessing[18] was applied to the data.

The structure of complex **3** was solved by direct methods and refined on F^2 using SHELXL 93.[19] The pentafluorophenyl rings and the methylene carbon atoms of one of the independent molecules in the asymmetric unit showed disorder. All were modelled for two sites with 50% occupancy. All non-hydrogen atoms except the fluorine and carbon atoms of the disordered phenyl rings were refined anisotropically. All hydrogen atoms were included in calculated positions (C–H 0.96 Å) with a fixed isotropic displacement parameter $1.5U_{eq}$(C) for the methyl groups and $1.2U_{eq}$(C) for the methylene groups.

The structure of complex **4** was solved by direct methods and refined on F^2 using SHELXL 93.[19] All non-hydrogen atoms were refined with anisotropic parameters. Three fluorine atoms of BF_4^- and the methylene carbon atoms showed disorder. All were modelled for two sites with 50% occupancy. All hydrogen atoms were included in calculated positions (C–H 0.96 Å) with a fixed isotropic displacement parameter $1.5U_{eq}$(C) for the methyl groups and $1.2U_{eq}$(C) for the remainder.

CCDC reference number 186/917.

See http://www.rsc.org/suppdata/dt/1998/1477/ for crystallographic files in .cif format.

Acknowledgements

We thank Dr. G. A. Griffith and R. Murphy for assistance with recording the NMR spectra, Dr. G. Eaton for recording the mass spectra and the Royal Society (E. G. H.) for support.

References

1 M. J. Atherton, J. Fawcett, J. H. Holloway, E. G. Hope, A. Karaçar, D. R. Russell and G. C. Saunders, *J. Chem. Soc., Chem. Commun.*, 1995, 191.

2 M. J. Atherton, J. Fawcett, J. H. Holloway, E. G. Hope, A. Karaçar, D. R. Russell and G. C. Saunders, *J. Chem. Soc., Dalton Trans.*, 1996, 3215.

3 G. B. Deacon, P. I. MacKinnon and T. D. Tuong, *Aust. J. Chem.*, 1983, **36**, 43; R. G. Finke, S. R. Keenan, D. A. Schiraldi and P. L. Watson, *Organometallics*, 1986, **5**, 598; 1987, **6**, 1356; M. J. Burk, D. L. Staley and W. Tumas, *J. Chem. Soc.*, *Chem. Commun.*, 1990, 809; O. Blum, F. Frolow and D. Milstein, *J. Chem. Soc.*, *Chem. Commun.*, 1991, 258; J. A. Marsella, A. G. Gilicinski, A. M. Coughlin and G. P. Pez, *J. Org. Chem.*, 1992, **57**, 2856; M. Aizenberg and D. Milstein, *J. Am. Chem. Soc.*, 1995, **117**, 8674.
4 S. Hintermann, P. S. Pregosin, H. Rüegger and H. C. Clark, *J. Organomet. Chem.*, 1992, **435**, 225.
5 P. Kebarle and S. Chowdury, *Chem. Rev.*, 1987, **87**, 513.
6 T. G. Richmond, C. E. Osterberg and A. M. Arif, *J. Am. Chem. Soc.*, 1987, **109**, 8091; C. E. Osterberg, M. A. King, A. M. Arif and T. G. Richmond, *Angew. Chem.*, *Int. Ed. Engl.*, 1990, **29**, 888; B. L. Lucht, M. J. Poss, M. A. King and T. G. Richmond, *J. Chem. Soc.*, *Chem. Commun.*, 1991, 400.
7 M. Crespo, M. Martinez and J. Sales, *J. Chem. Soc.*, *Chem. Commun.*, 1992, 822; M. Crespo, X. Solans and M. Font-Bardía, *Organometallics*, 1995, **14**, 355; O. López, M. Crespo, M. Font-Bardía and X. Solans, *Organometallics*, 1997, **16**, 1233; M. Crespo, M. Martinez and E. de Pablo, *J. Chem. Soc.*, *Dalton Trans.*, 1997, 1231.
8 R. L. Cook and J. G. Morse, *Inorg. Chem.*, 1982, **21**, 4103.
9 R. D. W. Kemmitt, D. I. Nichols and R. D. Peacock, *J. Chem. Soc. A*, 1968, 2149; D. I. Nichols, *J. Chem. Soc. A*, 1969, 1471; J. Fawcett, S. Friedrichs, J. H. Holloway, E. G. Hope, G. C. Saunders and A. M. Stuart, unpublished work.
10 C. Pelizzi and G. Pelizzi, *Acta Crystallogr.*, *Sect. B*, 1979, **34**, 1785.
11 M. J. Atherton, K. S. Coleman, J. Fawcett, J. H. Holloway, E. G. Hope, A. Karaçar, L. A. Peck and G. C. Saunders, *J. Chem. Soc.*, *Dalton Trans.*, 1995, 4029.
12 F. W. B. Einstein, X. Yan and D. C. Sutton, *Acta Crystallogr.*, *Sect. C*, 1991, **47**, 1975.
13 J. H. Holloway, E. G. Hope, K. Jones, G. C. Saunders, J. Fawcett, N. Reeves, D. R. Russell and M. J. Atherton, *Polyhedron*, 1993, **12**, 2681.
14 A. D. U. Hardy and G. A. Sim, *J. Chem. Soc.*, *Dalton Trans.*, 1972, 1900; R. L. Cook and J. G. Morse, *Inorg. Chem.*, 1984, **23**, 2332; M. F. Ernst and D. M. Roddick, *Inorg. Chem.*, 1990, **29**, 3627.
15 M. J. Atherton, J. Fawcett, J. H. Holloway, E. G. Hope, D. R. Russell and G. C. Saunders, unpublished work.
16 gNMR, version 3.6, Cherwell Scientific Publishing Ltd., Oxford, 1995.
17 G. M. Sheldrick, SHELXL 96, Program for Crystal Structure Refinement, University of Göttingen, 1996.
18 R. H. Blessing, *Acta Crystallogr.*, *Sect. A*, 1995, **51**, 33.
19 G. M. Sheldrick, SHELXL 93, Program for Crystal Structure Refinement, University of Göttingen, 1993.

Received 19*th January* 1998; *Paper* 8/00515J